

Springer Controlled Release Society Book Series on Advances in Science and Technology: Analytical Techniques in Pharmaceutical Sciences, Section 5 Imaging techniques, Chapter 21 Applications of AFM in pharmaceutical sciences, T. Rades, A. Mullertz and Y. Perrie (Eds.), (2014), in press.

Section 5: Imaging techniques

Chapter 21: Applications of AFM in Pharmaceutical Sciences

Dimitrios A. Lamprou^{1,*} and James R. Smith²

¹*Strathclyde Institute of Pharmacy and Biomedical Sciences (SIPBS), University of Strathclyde, 161 Cathedral Street, Glasgow G4 0RE, UK.*

²*School of Pharmacy and Biomedical Sciences, University of Portsmouth, St Michael's Building, White Swan Road, Portsmouth PO1 2DT, UK.*

*Corresponding author: dimitrios.lamprou@strath.ac.uk

Table of contents

1. Introduction
 - 1.1. Background
 - 1.2. Principles of operation
 - 1.3. Operating modes
 - 1.4. Cantilevers and tips
 - 1.5. The need for AFM in pharmaceutical research
2. Use of AFM in pharmaceutical sciences
 - 2.1. Tablet coating and dissolution
 - 2.2. Crystal growth and polymorphism
 - 2.3. Particles and fibres
 - 2.4. Nanomecidine
 - 2.5. Nanotoxicology
 - 2.6. Drug-protein and protein-protein interactions
 - 2.7. Live cells
 - 2.8. Bacterial biofilms
 - 2.9. Viruses
3. AFM combined with optical or spectroscopic techniques
4. Summary

Appendix: Obtaining an AFM contact mode image in air

References

1. Introduction

Atomic force microscopy (AFM) continues to find ever wider applications in the fields of materials characterisation and life sciences. By using a small tip to scan across the sample's surface, the requirement to focus light and electrons as with light and electron microscopies is eliminated; this overcomes the Rayleigh criterion resolution limit, enabling nanometre and sometimes atomic resolution imaging, depending on the sample and / or imaging regime, to become routine. AFM can be operated without the need for conducting or stained samples and therefore can be operated in physiological media. Further, the probe can be used to push into or pull away from sample surfaces, yielding quantitative nanomechanical and adhesion data, which can also be displayed graphically. This chapter will discuss the fundamentals of AFM and highlight a few recent applications with relevance to pharmaceutical science.

1.1 Background

The atomic force microscope (AFM; scanning force microscope, SFM) is the principal member of a number of related scanning probe microscopes (SPM). The first of these was the scanning tunnelling microscope (STM), invented by Binnig and Rohrer, whom received the Nobel Prize for Physics, in 1982 after revealing the first atomic resolution images (Binnig and Rohrer 1982). By applying a bias potential across a small gap between a sharp metallic tip and a conducting sample, it was possible for electrons to tunnel across the forbidden energy gap; if the probe was simultaneously scanned across the sample, the tunnelling current yielded an image related to the topography (strictly, the local density of states) of the sample. The technique necessitated the use of conducting specimens, with the exception of DNA, proteins and other small molecules, and so was restrictive for the study of thicker biological samples and other insulating materials, such as polymers. To overcome this issue, the imaging method was developed, by the same inventors, to measure forces on a cantilever, to which the tip was mounted, rather than tunnelling currents: this became the AFM instrument (Binnig et al. 1986). In 1992, SPMs capable of both STM and AFM, became commercially available and very soon afterwards a vast array of derivative techniques and modes, almost solely AFM-based, were developed. AFM has finally come of age, with new imaging modes and related techniques continually coming to market; highlights of these are summarised later in this chapter.

1.2 Principles of operation

Before discussing the multitude of acquisition modes, some of the fundamentals of AFM will be presented. AFM operates by scanning a small, usually square pyramidal shaped tip, prefabricated onto a cantilever, across a sample, mounted on a stub, which is magnetically held into place on top of a piezoelectric ceramic scanner. Piezoelectric crystals change shape on the application of a voltage, the relationship being roughly proportional and accurate to 0.1 Å; it is this feature that provides AFM with its high resolution capability. The piezos are arranged in the scanner (tripod or the more usual tube design) to provide x, y and z (height) movement, the former two of which allow the scanning motion. The arrangement here describes a sample-scanning rather than tip-scanning instrument, i.e., the sample scans a stationary tip. It is often more convenient, however, to imagine the tip scanning the sample, as will be discussed here.

The cantilever is often coated with a gold layer to make it reflective, so that a laser can be reflected from the cantilever onto a photodetector, via a mirror (Figure 1). This laser assembly serves as a tracking system so that the position of the tip in relation to the surface can be continuously monitored. In contact mode, the simplest of operations, the probe (tip + cantilever) is brought into contact with the sample until a small deflection of the cantilever, corresponding to a repulsive force (the set-point), is detected via a displacement on the photodetector. The probe is then scanned across the surface causing the cantilever to move vertically corresponding to variations in topography (height) of the sample. As the probe begins to go over a high feature on the specimen, for example, the cantilever will start to deflect more (bending will increase) causing the laser spot on the photodetector to move. So as not to cause damage to the sample, and / or tip, a voltage signal from the photodetector is sent to the scanner, to which the sample is mounted, causing the scanner to retract. This then lowers the sample, relieving the increased deflection (above the set-point) on the cantilever. Upward movement of the piezo, and sample, is also allowed when, for example, the probe moves over a low feature, such as a pit. This cycle is repeated as the sample is scanned, so that the deflection of the cantilever is kept constant by means of this feedback loop. The potential required to maintain the set-point via the feedback circuit is used, alongside the x and y coordinates, to create the contact mode AFM image. Some practical steps on how to acquire contact mode images are given in the Appendix.

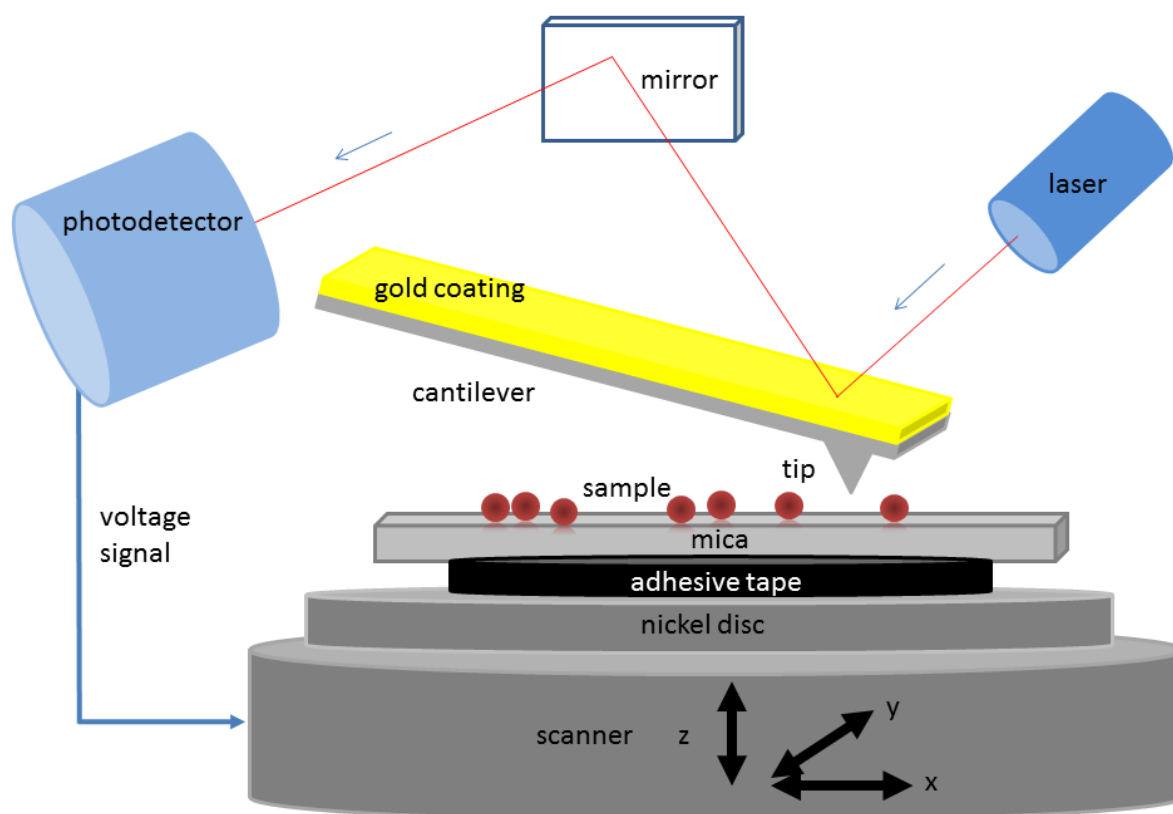


Figure 1. A schematic of the main components of a typical AFM, with particles on a mica surface.

1.3 Operating modes

There are three operating modes in AFM: contact mode, Tapping Mode® (a trade mark of Bruker, and also known as intermittent contact mode) and non-contact mode. The last two modes are referred to as 'ac' techniques while contact mode is referred to as 'dc'. Each has their own advantages and disadvantages. Contact mode is the simplest, where the cantilever moves along the surface maintaining a set force. If too much force or too little force is detected, the height will be adjusted using the piezoelectric motors through the feedback loop (Section 1.2). Tapping Mode® is probably as widely encountered as contact mode. Here, to minimise potentially damaging lateral forces being exerted on the sample, the cantilever is oscillated at its resonant frequency during scanning; the measurement is made only at the moment when the tip touches the specimen, and for the most part, while the scanner moves the sample, the tip is safely retracted. Tapping Mode® is often used for imaging delicate biological samples, such as DNA, and this can also be carried out in physiological media.

With most commercial instruments, different image channels can be acquired at the same time as the topography (height) image. For example, in contact mode, the error signal (raw signal detected by the photodetector) and the friction response (or lateral force microscope, LFM image, derived from the horizontal component of the photodetector's signal as the cantilever twists during scanning) may be obtained. Similarly, in Tapping Mode®, in addition to the error signal, the phase image (not to be confused with other definitions of this term in microscopy) and amplitude image may be obtained (Schmitz et al. 1997). These respectively correspond to the time (phase) lag and amplitude of the driven tapping sine wave signal relative to the response wave after interacting with sample. For example, variations in viscoelastic and / or adhesion properties of the sample across the surface may modify the phase and / or amplitude signals. These modes often give more defined visual contrast than their simultaneously acquired topography images, although the exact mechanism behind their complex origin is rarely understood.

In addition to imaging, force data can be obtained by pushing the tip into or pulling the tip away from a sample's surface; this is often referred to as force spectroscopy (Butt et al. 2005). This can be explained with reference to a force vs. distance plot (force curve; Figure 2), where a tip approaches a surface, typically experiences a short-range attraction event and then is pushed into the surface (Cappella and Dietler 1999; Butt et al. 2005). The gradient of the force curve in this region is a combination of indentation of the tip into the sample and cantilever bending, and with a suitable hard reference surface and use of mathematical models, quantitative nanoindentation (Young's modulus) data can be extracted. After a user-defined selected total force (or deflection), the applied load on the cantilever can be reduced, and the tip may eventually become adhered to the surface. Overcoming this force leads to an adhesion event, the importance of which becomes significant when the tip is suitably chemically derivatised or biologically functionalised (Section 1.4). Typically, only one-half of the force curve (an approach or retract curve) is relevant for any given experiment.

Nowadays, force measurements are combined with the scanning capability to produce local physical property maps, e.g., indentation, Young's modulus, adhesion and friction. These can be quantitative or qualitative depending on the extent of pre-calibration. Instrument

manufacturers tend to have their own trade mark names for these modes, such as Torsional Resonance (TR) Mode® and PeakForce Tapping® (PFT).

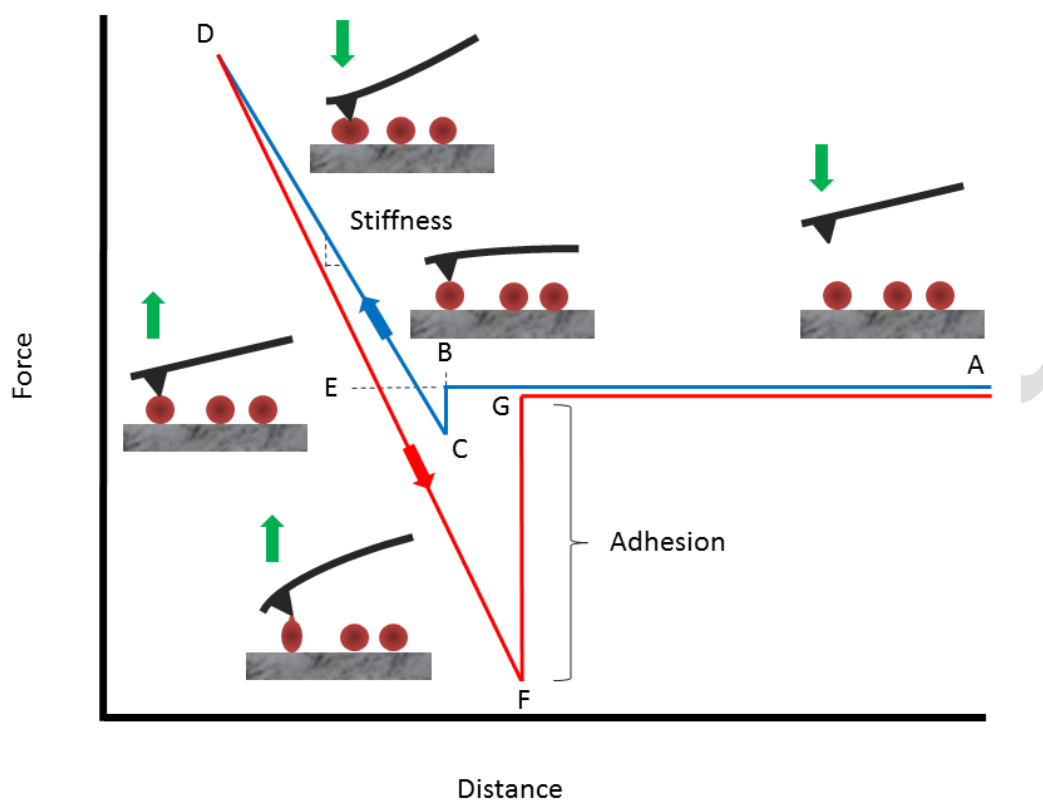


Figure 2. A schematic showing the some key features of an AFM force vs. distance plot: Blue line: approach curve, red line: retract curve; regions A-B: tip approaches the surface, B-C: tip-surface attraction, C-D: tip driven into the surface combined with cantilever bending (where stiffness / compliance information may be extracted), D: point at which applied load is withdrawn and tip pulled away from the surface, E: no net attractive or repulsive forces between tip and sample, E-F: tip is adhered to sample, F: applied load overcomes adhesion force and tip released from surface (maximum adhesion force), F-G: adhesion force, G: tip away from surface, G-A: continued withdrawal of the tip.

In the TR mode, the tip is parallel rather than vertical to the surface, and the forces between the tip and the sample cause a change in resonance behaviour that can be used to track the surface at a constant distance. The TR mode has the advantage that the tip remains at a constant distance from the surface at all times. Song and Bhushan (2006) investigated the dynamics of the tip-cantilever system when it is operated in TR mode, with or without tip-sample interaction, and they also described the basic methodology to extract in-plane surface properties in TR mode.

PFT is similar to Tapping Mode® AFM, however the PFT oscillation is performed at frequencies well below the cantilever resonance and the force on the tip can be kept constant which differs from Tapping Mode® AFM where the probe vibration amplitude is controlled by the feedback loop. A continuous series of force-distance curves is produced and by keeping the peak force constant, the modulus, adhesion force, and deformation depth can be

calculated. In PFT, the oscillation combines the benefits of contact and Tapping Mode® imaging by having direct force control and avoiding damaging lateral forces. PeakForce Quantitative Nanomechanical Mapping (QNM®) (Bruker) is a recent and powerful technique that provides quantitative characterisation of surfaces at the nanoscale level (Lamprou et al. 2013). Individual force curves can be acquired and quantitatively analysed as the tip taps across the surface.

By attaching a ligand onto the tip, it is possible to map receptor-binding sites on cell / substrate surfaces, with a lateral resolution of a few nanometres, whilst simultaneously acquiring the topography image; this is known as topography and recognition imaging (TREC) mode or single-molecule force spectroscopy (SMFS), a single-molecule interaction method (Ebner et al. 2010; Muller et al. 2009).

Outside the scope of this short chapter lie a whole host of related probe techniques (not strictly modes). These, as their names suggest, are able to obtain other local physical properties; they include electrochemical AFM (EC-AFM), magnetic force microscopy (MFM), electrostatic force microscopy (EFM), kelvin probe force microscopy (KPFM), photoconductive AFM (pcAFM), scanning spreading resistance microscopy (SSRM), scanning thermal microscopy (SThM), scanning capacitance microscopy (SCM) and surface potential microscopy (SPoM).

Some of the latest developments include fast scanning, where the typical 1 Hz scan rate (ca. 10 min per scan) can be rapidly increased, and in some cases, for flat samples, to real-time acquisition. This is achieved through the use of small cantilevers.

1.4 Cantilevers and tips

A wide variety of cantilevers and tips (often jointly named probes, although terms are used interchangeably) are available depending on their intended application. Broadly, contact mode probes tend to be made from silicon nitride, a hard material of approximate stoichiometry Si_3N_4 , whereas Tapping Mode® probes are normally formed from silicon, owing to its stiffness, although Si_3N_4 is also sometimes used.

The shapes of the cantilevers also vary, for example, V-shaped (often used for contact mode), beam-shaped (rectangular) and arrow shaped. The cantilever's spring constant (k , N m^{-1}), a proportionality constant used to relate cantilever deflection to force, can be determined from the dimensions (typically, 10 – 450 μm in length and various widths) and material properties of the cantilever. There are numerous methods for measuring k , such as the thermal noise method, described elsewhere (Clifford and Seah 2005, Lamprou et al. 2010). Accurate determination of this property, for which manufacturers provide approximate ranges, is essential for all AFM studies where force measurements are required.

The tip itself can be a square pyramid (approximating at its apex to a small sphere, the radius R of which may need to be determined for some force measurements), an oxide-sharpened tip (small R), a high-aspect ratio tip or a colloid probe. The latter type includes small entities, such as cells or polymer spheres that can be adhered to a tip-less cantilever to bestow biological functionality or defined contact geometries.

Probes can also be coated on either side for increased laser reflection (top side: Au), chemical functionalisation (underside: Au) or to change physical properties (underside: Pt, diamond-like coatings, magnetic Co alloys). Chemically modified probes are typically prepared by grafting thiol self-assembled monolayers (SAMs) on to Au coated probes or by silanising the surface OH groups of Si / Si₃N₄ probes, which are then used to measure specific short-range intermolecular (usually adhesion) forces. This is often termed chemical force microscopy (CFM; Smith et al. 2003a). Florin et al. (1994) first used functionalised AFM tips and surfaces to measure forces between biotin-avidin ligand-receptor pairs; this area has now been extended to investigate many interacting pairs.

Many different approaches have been used to attach (bio)molecules to AFM probes. For example Sikora et al. (2012) used AFM to investigate protein-protein (the core methylase and the HsdR subunit) interactions within the EcoR124I molecular motor. To do this, they functionalised a tip with a glutathione S-transferase-HsdR complex via a NHS-PEG-MAL linker and probed the core methylase (Figure 3). The NHS end of the PEG linker reacts with amines on an amino-terminated, silanised Si₃N₄ tip, forming a stable amide bond, while the MAL group forms a C-S linkage with the protein. Li et al. (2013b) used a similar linker to attach the drug rituximab to an AFM tip.

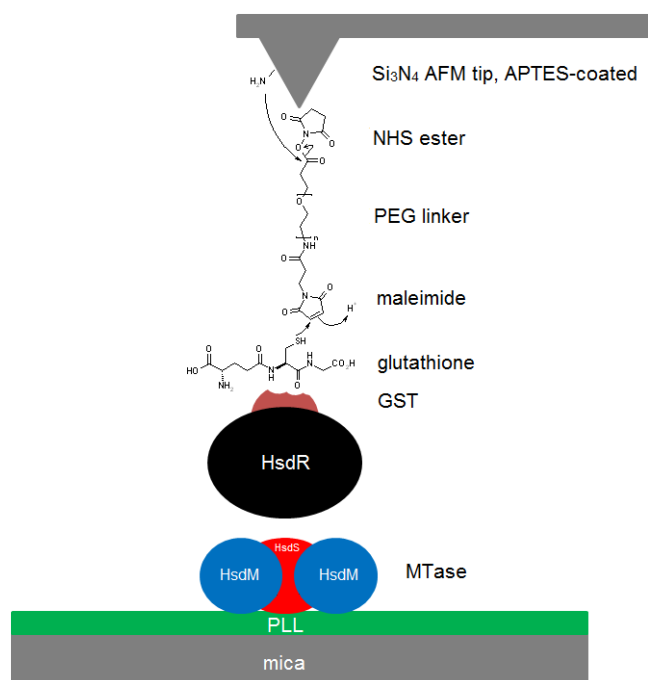


Figure 3. Surface chemistry used to immobilise proteins to a Si₃N₄ AFM tip and a mica surface to study protein-protein interactions, in this case different subcomponents (HsdR / HsdS / HsdM) of a molecular motor (type I restriction-modification enzyme EcoR124I). APTES = (3-aminopropyl)triethoxysilane (to form surface NH₂ groups), PLL = poly(L-lysine) (a polycation to couple proteins to negatively charged mica), GST = glutathione S-transferase. Reproduced with permission (Sikora et al. 2012).

Riener et al. (2003) developed an 'easy-to-use test system' for investigating single ligand-detectors with AFM, demonstrating this using the avidin-biotin interaction where the AFM tip was biotinylated via a 6 nm PEG linker. Hinterdorfer et al. (1996) functionalised a tip with an antibody via an 8 nm PEG linker and an amino-functionalised Si_3N_4 . Cail and Hochella (2005) added a polystyrene micro-bead to a cantilever to investigate sticking efficiency in colloid systems; spheres were simply glued to the cantilevers with UHU 5-minute epoxy glue. The procedure was carried out by placing a tip-less Si_3N_4 cantilever in the AFM apparatus, using the piezoelectric actuators to drive the cantilever into the adhesive and then onto a glass slide covered with microspheres and picking up a single microsphere.

1.5 The need for AFM in pharmaceutical research

The potential of AFM for structural biological studies was recognised since the conception of the technique. Indeed, it was the inability of tunnelling currents in STM to penetrate through the thickness of biological specimens greater than the diameter of proteins that led to the realisation of AFM. Nowadays, with the multitude of operating modes available, including the ability for real-time imaging in physiological buffer, many questions of interest to those engaged in pharmaceutical research can be answered. For example, ligand-receptor binding on cell surfaces can be measured and mapped, protein-protein interactions can be studied to provide kinetic information and AFM shows potential for use as an early diagnostic tool for cancer and other diseases.

The remainder of this chapter is dedicated to outlining selected examples that highlight the application of AFM in pharmaceutical research, ranging from coatings characterisation through to nanotechnology and biological applications. Many of these investigations have been from the past four years, both from the literature and a few from the authors' laboratories.

2. Use of AFM in pharmaceutical sciences

2.1 Tablet coating and dissolution

Pharmaceutical solid dosage forms are usually coated to control drug release, to protect active pharmaceutical ingredients (APIs) from degradation in the stomach or in humid atmospheres, to provide a barrier to taste and smell, and for controlling dissolution (Romer et al. 2008). AFM has been used mainly to acquire topography information, where it has the advantage over SEM in that it can provide quantitative surface roughness and surface area measurements and allow for their study in real-time (Seitavuopio et al. 2005); data on compositional distribution and porosity may also be discerned. Seitavuopio et al. (2003) investigated tablet surfaces using different imaging and roughness techniques, including AFM, and concluded that KCl tablets were smoother than NaCl tablets. A summary of surface roughness parameters that can be readily obtained from AFM topography profiles has been described by Smith et al. (2003b).

The coating materials of tablets are frequently studied as free films so that the effects of the tablet core can be eliminated (Kwok et al. 2004). Seitavuopio et al. (2006) used AFM imaging to examine the surfaces of pharmaceutical tablets that were coated with different aqueous hydroxypropyl methylcellulose films. AFM has been used to assess the quality of

montmorillonite / poly(styrene) / poly(butyl acrylate) films prepared using dispersion methods (Csontos et al. 2006); the influence of composition on the form and arrangement of polymer droplets, and also the uniformity of the polymer film surface on the tablets were investigated. AFM can also be used to investigate areas on surfaces that have different properties, such as crystallinity and chemical composition; these are important parameters concerning the dissolution of a tablet.

The mechanisms and dissolution rates of the cholesterol monohydrate (001) surface, of relevance to the removal of gallstones, were investigated by Abendan and Swift (2005). The dissolution rate was found to be closely related to local variations in topography. Danesh et al. (2001) measured the dissolution rates of the (001) and (100) planes of aspirin crystals (0.45 and 2.93 nm s^{-1} , respectively) in 0.05 M HCl . The (001) crystal plane dissolved by receding step edges, whilst the (100) surface showed crystal terrace sinking. Such studies are important as in vitro crystal dissolution is proportional to in vivo drug absorption (Levy 1961).

2.2 Crystal growth and polymorphism

Drug crystal growth, particle characterisation and tablet coatings are critical elements in the manufacture of solid dosage forms. Thus, microscopic examination is important for the design and evaluation of a pharmaceutical product after the steps in the drug formulation process have been taken.

AFM was first introduced into crystal growth studies by Durbin and Carlson (1992), who detected the growth of steps on the surfaces of lysozyme crystals. Tonglei et al. (2000) used AFM for monitoring the crystal surface and they reported the step velocity of egg-white lysozyme crystal planes on a nanometre-scale using a sealed vessel in the AFM and noted the consequences of controlling the supersaturation. Land and De Yoreo (2000) used an in situ AFM for investigating the growth and activity of dislocation sources as a function of supersaturation during canavalin crystal growth. They reported that growth occurs on monomolecular steps generated either by simple or complex screw dislocation sources, and also visualised 2D nucleating islands that form onto the surface before spreading laterally as step bunches. Onuma et al. (1995) used AFM to investigate the topography of hydroxyapatite single crystals that had been synthesised from hydrothermal solution, and reported that growth proceeded through a layer-by-layer mechanism. Miyazaki et al. (2011) determined crystal growth rates of nifedipine at the surface of amorphous solids with and without polymers using AFM; they found the technique to be useful for studying the crystallisation kinetics of amorphous solids by targeting the crystals at the surface. Thompson et al. (2004), utilised AFM to assess the growth on the (001) face of aspirin crystals at two supersaturations, elucidating both the growth mechanisms and kinetics at each supersaturation. They also assessed the capability of AFM to follow the structural transformations of crystals that can occur in unstable pharmaceutical compounds. Thakuria et al. (2013) used AFM to observe the phase changes at crystal surfaces where the transformation is supplemented by changes in the spacing between layers of molecules. They analysed the thermodynamically stable form of the caffeine-glutaric acid cocrystal continuously in situ using intermittent-contact mode AFM. Further information on the applications of AFM for the visualisation of crystal growth can be found in two review papers by McPherson et al. (2001) and Chow et al. (2012).

Different polymorphs have different physicochemical properties, which could affect the solubility, dissolution and stability, and therefore polymorphic characterisation is an important parameter in pharmaceutical industry. AFM can be applied both in situ and ex situ to study the growth of crystals from solution, and in particular for investigating the crystallisation of proteins, nucleic acids and viruses (McPherson et al. 2001). Yip and Ward (1996) used AFM to identify the polymorphic forms of insulin and Danesh et al. (2000) mapped the distribution of polymorphs on the drug cimetidine. The author's group (DL) have investigated the nanocrystalline growth of dibenz[a,c]anthracene using a FastScan AFM (Figure 4).

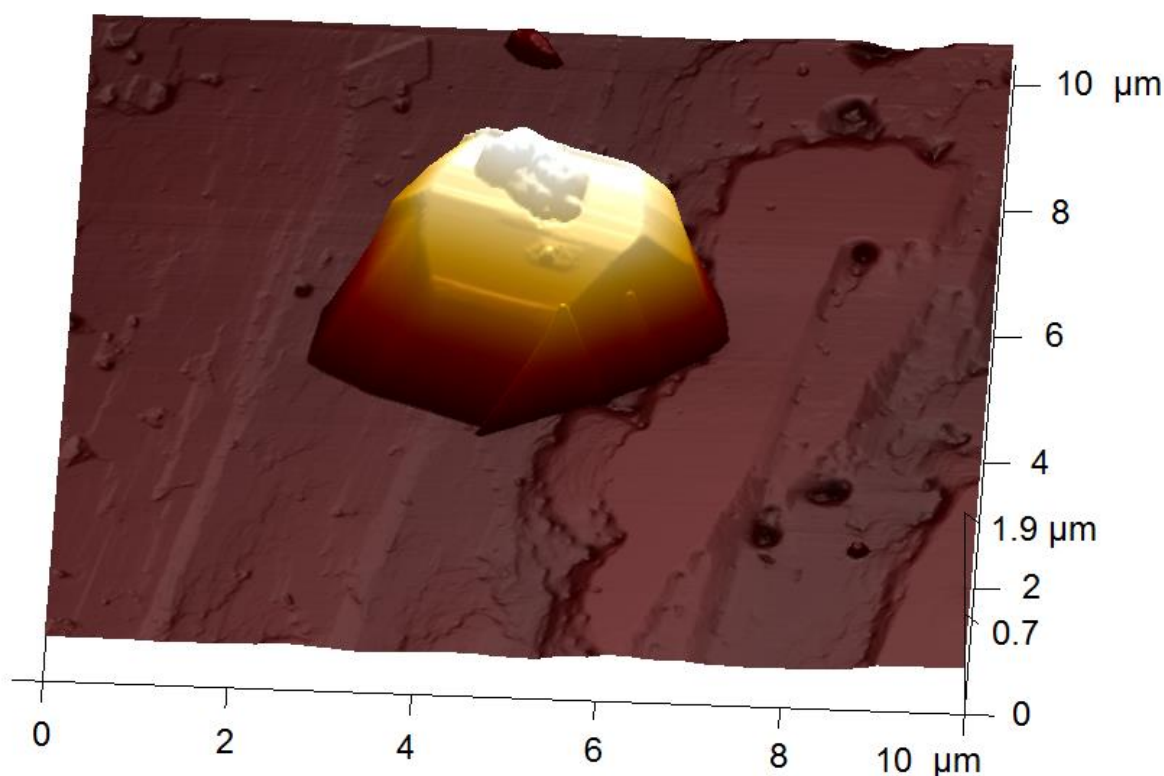


Figure 4. AFM image of a dibenz[a,c]anthracene crystal grown on top of a similar structure crystal.

2.3 Particles and fibres

AFM offers particular advantages over TEM and SEM for the characterisation of particles and fibres, such as height measurement, minimal sample preparation, the ability to operate under atmospheric pressure and in liquids, and the acquisition of nanomechanical / adhesion data. These advantages facilitate the study of loaded and empty delivery systems.

AFM is an excellent technique for visualising particles with sizes ranging from 1 nm to 10 µm, allowing quantitative particle size measurements. These are not prone to problems experienced when using SEM, such as conducting coating thickness, astigmatism, penetration

depth and absence of height information. SEM and dynamic light scattering (DLS) may also cause slight deformations of soft particles, such as liposomes (Figure 5; Onyesom et al. 2013). Since x, y and z distances may be recorded using AFM, parameters such as diameter, volume and surface area can be calculated. AFM is one of the most important techniques for the characterisation of lipid drug delivery systems (Potta et al. 2011), which have been successfully used as drug carriers for the treatment of many cancers.

Recently, AFM has been used to study the scale-up and shelf-stability of curcumin-encapsulated poly(lactic acid-co-glycolic acid) (PLGA) nanoparticles (NPs), which were found to be stable for periods up to 6 months; the particles were spherical and had smooth surfaces (Grama et al. 2013). AFM has been also used to characterise Au NPs with sizes 25, 55 and 90 nm, for investigating the stability of the naked, PEGylated, and Pt-conjugated NPs as a function of time under various conditions (Craig et al. 2012).

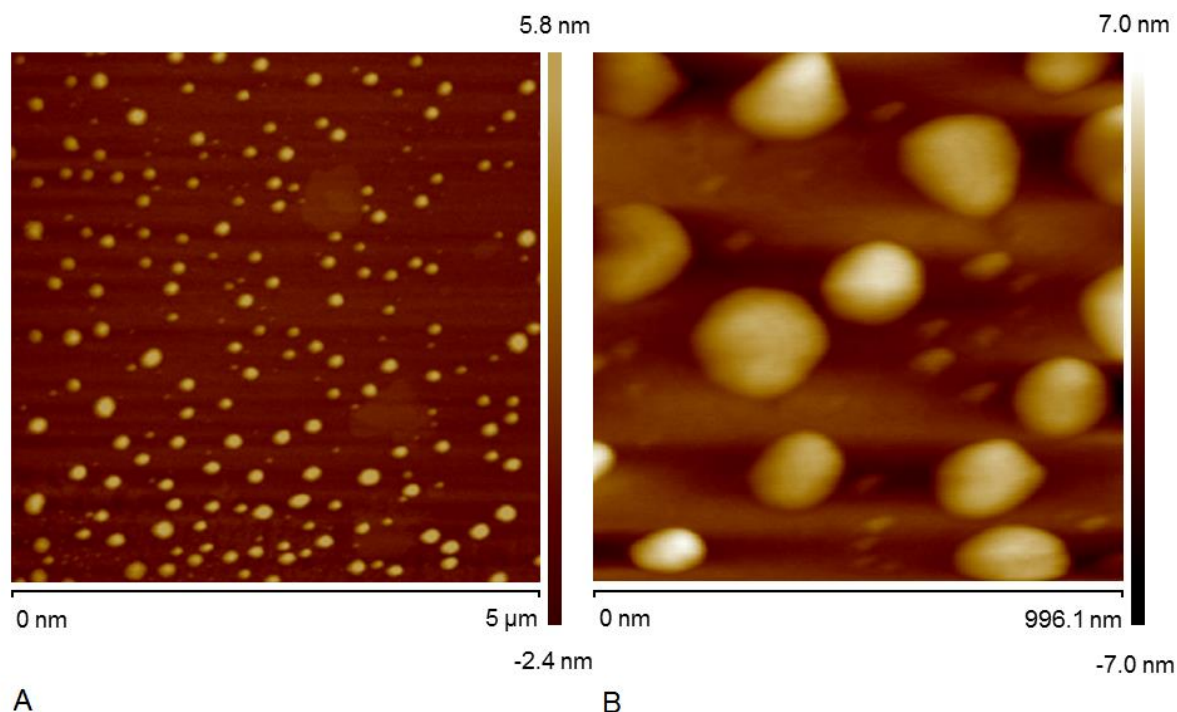


Figure 5. AFM topography images (using PeakForce QNM® mode in air) of cholesterol-stabilised, dipalmitoylphosphatidyl choline (DPPC) Stealth liposomes. A, unloaded, B, sirolimus-loaded. Reproduced with permission (Onyesom et al. 2013).

Tsukada et al. (2004) developed AFM colloid probe techniques to mount a 1 – 3 µm spherical polycrystalline drug particle on a cantilever to measure adhesion to an α -lactose monohydrate layer for developing formulations for dry powder inhalers (DPI). Begat et al. (2004) used a similar arrangement to investigate adhesive and cohesive force characteristics of DPI systems containing budesonide or salbutamol sulphate to α -lactose monohydrate.

AFM has recently been used for the analysis of amyloid fibrils, an important research area in diseases such as Parkinson's, Alzheimer's, and type II diabetes (Chiti and Dobson 2006). For example, Mains et al. (2013) used drug-loaded lysozyme amyloid hydrogels, prepared by misfolding lysozyme in the presence and absence of drugs, such as atenolol, propranolol hydrochloride or timolol tartrate (Figure 6). Different amyloid fibre structures were formed depending on the type of drug used. Josef and Mezzenga (2012) stated that AFM can contribute to research of amyloid fibrils by providing important information concerning fibril structure and fibrillation processes, and also to analyse some important properties of amyloid fibrils, such as their strength and Young's modulus. The contour length is also a very useful structural parameter of amyloid fibres that can be determined from AFM imaging; the property can be used to interpret the cellular response to the presence of amyloid fibrils of different sizes after fragmentation. Shorter fibrils have been found to have enhanced cytotoxicity compared to longer fibrils (Xue et al. 2009).

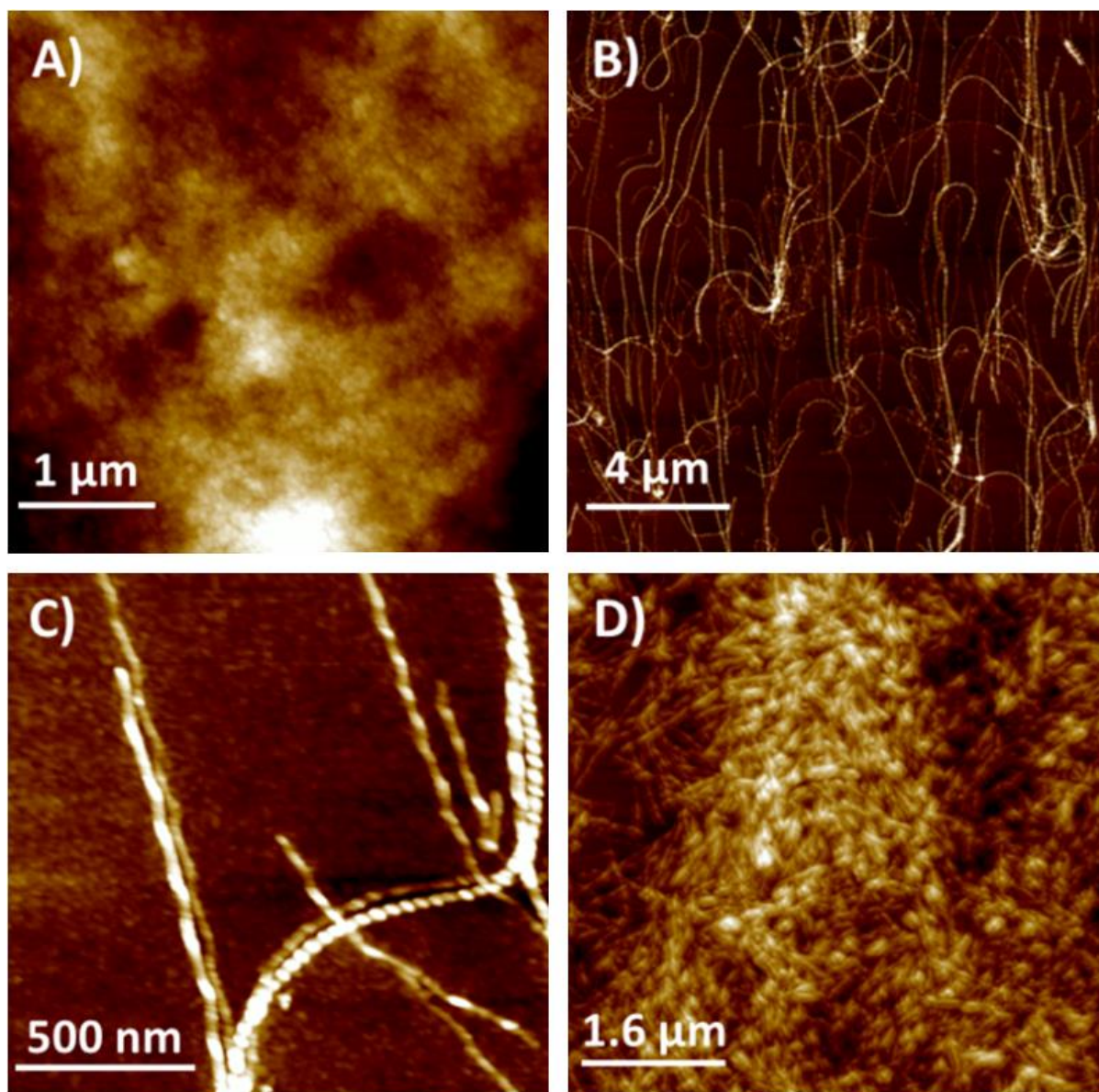


Figure 6. AFM height images of drug loaded amyloid hydrogels. Drugs: A, atenolol; B, propranolol; C, propranolol, with image showing both long and short range periodicity fibres; D, timolol. Reproduced with permission (Mains et al. 2013).

2.4 Nanomedicine

Nanomedicine is an interdisciplinary field encompassing the detection, prevention and treatment of diseases at the nanometre scale (Karagkiozaki et al. 2012), which includes the longer terms goals of producing personalised medicines (Janowski et al. 2012). Materials used in this application area include polymer coatings and nanoscale drug delivery devices, respectively, recently reviewed by Smith and Lamprou (2014) and Sitterberg et al. (2010), the latter of which focuses exclusively on the use of AFM.

AFM phase imaging, in conjunction with TEM and other techniques, has been used to characterise PEGylated lipoplexes for siRNA drug delivery (Belletti et al. 2013). Post-PEGylation was found to yield improved homogeneity with regards to PEG coverage. Karagkiozaki et al. (2013) used Tapping Mode® AFM to assess the morphology, surface roughness and cytocompatibility of conducting polymers as nanocoatings for tissue regeneration for cardiovascular implants. The use of these materials for this type of application has been recently reviewed (Smith and Lamprou 2014).

The size and morphology of liposomes for transporting boronated compounds for use in boron neutron capture therapy (BNCT) for targeted cancer treatments have been investigated by Tapping Mode® AFM (Theodoropoulos et al. 2013). Carbon nanotubes show promise as drug delivery devices owing to their dimensions, biocompatibility and ease of chemical functionalisation (Bianco et al. 2005). Tapping Mode® AFM has been used to show lipids wrapped around single-walled carbon nanotubes to increase their dispersion in aqueous media (Tasis et al. 2008; Roldo et al. 2009; Wise et al. 2008).

Adhesion forces between hematite NPs and *E. coli* immobilised onto a tip-less cantilever have been measured in phosphate buffer solution (Zhang et al. 2011). This fundamental study investigated the interaction forces and contact mechanics of the system, and a new model to describe the interaction was devised.

Lamprou et al. (2013) investigated the use of PeakForce QNM® for improving the developments in the field of nanomedicines, by measuring the effect of particles into various tissues (e.g., liver, kidney and small intestines). They also described how this detailed imaging approach may also help scientists address growing concerns in nanotoxicology.

2.5 Nanotoxicology

Nanotoxicology is a relatively new field, developed to study the toxicological effects of NPs (natural or engineered) / nanomaterials in the environment, which can differ markedly from their bulk materials due to their small particle size and large surface area (Donaldson et al. 2004). With the rapidly increasing use of nanomaterials, currently over 1000 commercial products, there is an urgency to determine their toxicity and to control exposure (Arora et al.

2012). There are a number of in vitro techniques that can be used for testing, such as proliferation assays, reactive oxygen species (ROS) generation analysis, flow cytometry, DNA damaging potential assays, gene expression analysis, genotoxicity and microscopic evaluation, including SEM / EDAX, TEM, fluorescence microscopy, MRI and AFM (Arora et al. 2012). Chinnapongse et al. (2011) used AFM to investigate the persistence of citrate-capped Ag NPs (20 nm) in natural freshwaters and synthetic aquatic media. Tetard et al. (2010) observed single-walled carbon nanohorns and SiO₂ NPs buried in cells using various AFM oscillation techniques. The morphology and particle size of TiO₂ NPs, which are being increasingly used in catalysis and as a pigment, were characterised by Thio et al. (2011). The nanotoxicological effects of graphene on human plasma were studied by Mao et al. (2013), who found low molecular weight proteins to have a high affinity for the nanomaterial. Parallel investigations found decreased nuclei numbers and increased ROS after prolonged incubation with Hela and Panc-1 cell lines.

2.6 Drug-protein and protein-protein interactions

The study of protein-protein and drug-protein interactions represents one of the most important topics in the field of pharmaceutical sciences and is critical for targeting drug delivery (Edwardson and Henderson 2004). Proteins can be used as adapters conjugated to NPs (chitosan, Au, liposomes, silica, self-assembly) for targeting drug delivery. Furthermore, the interaction between protein molecules with drug carriers and cell surfaces is crucial (Bastatas et al. 2012), since cell adhesion to surfaces depends on the availability of specific protein-binding sites. Protein-material interactions also play a significant role in biosensors as a diagnostic tool since ligands can be immobilised on a probe surface and used to analyse the corresponding integrin. In addition, proteins encounter a wide range of surfaces during processing, each of which has the potential to affect their structure if adsorption takes place. If a loss of structure takes place upon surface adsorption, or even a small change in the native fold, subsequent protein-protein interactions may occur, resulting in the formation of aggregates and thus potentially an immunogenic response. Roberts (2005) identified challenges that need to be addressed when AFM adhesion measurements are to be used to study single drug particles interacting with proteins or cells. Couston et al. (2012) studied the interactions between monoclonal antibodies and albumin to surfaces of varying functionality and hydrophobicity by monitoring the adhesion over time and found a two-step interaction process involving an initial, rapid perturbation of the protein surface on contact with the surface, followed by relaxation and unfolding. Fahs and Louarn (2013) investigated the nanomechanical and adhesion properties of 2S albumin and 12S globulin. Differences in tip-protein interaction strength with regard to the nature of the protein and pH of the aqueous environment in terms of protein unfolding were observed. Protein-protein interactions have been studied also by Kao et al. (2012), where B-cell / CD80 was immobilised on an AFM tip and T-cell / CD28 was immobilised to a surface and forces were measured before and after adding cynarine.

2.7 Live cells

The ability to image, probe ligand-receptor interactions and obtain nanomechanical information, all in physiological media, makes AFM particularly suited for studying cells in a therapeutic context.

Kozlova et al. (2013) obtained contact and intermittent contact mode images of the surfaces of red blood cells (RBCs) that had been treated in vitro with various agents (hemin, furosemide, chlorpromazine and zinc ions) to investigate blood intoxication. Images were filtered using a Fourier transform algorithm to detect poorly seen structures on RBC membranes. The study showed that blood intoxication affected the nanostructures present on the RBC membrane surfaces.

Surface roughness has been suggested to provide a diagnostic measure the health state of cells (Antonio et al. 2012). Widespread application of this method has been limited by scan-size dependence on surface roughness, although this has been overcome by the work of Antonio et al. (2012).

Li et al. (2013a) used SMFS to map CD20 molecules on surfaces of cancer B cells (fluorescently labelled; mapped area $500 \times 500 \text{ nm}^2$) obtained from patients with B-cell non-Hodgkin's lymphoma (NHL; marginal zone lymphoma; Figure 7). CD20 can be targeted therapeutically with monoclonal antibodies (mAb), such as rituximab. These antibodies were covalently linked to an AFM tip via silanisation and a PEG linker; the density was such that only one CD20-rituximab complex was formed per force curve. RBCs, which do not express CD20, were used as controls. These studies are useful in understanding mechanisms, and developing new anti-CD20 mAbs especially where rituximab resistance becomes a problem.

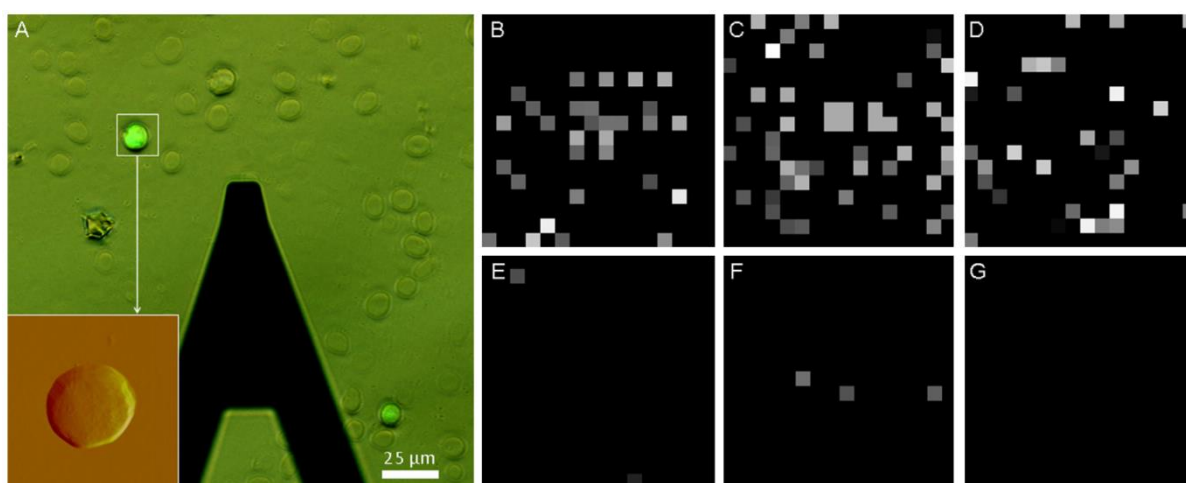


Figure 7. Measuring specific CD20-rituximab interactions on cancer cells using a rituximab functionalised tip. A, Bone marrow cancer B cells fluorescently labelled for easy identification; B-D, CD20 distribution map (xy: $500 \times 500 \text{ nm}^2$, z: 0 - 100 pN, 16×16 pixels); E-G, CD20 distribution map after blocking (same scale). Reproduced with permission (Li et al. 2013a).

Numerous nanoindentation studies of cells have appeared in the literature, many describing differences in elastic behaviour between cancer cells and benign equivalents (Cross et al. 2007; Li et al. 2008), where the Young's modulus of the affected cells is often cited as being ca. 70% less stiff than non-cancerous cells (Cross et al. 2007). The differences are usually

attributed to rearrangements in the cytoskeleton network and have been suggested to be of early diagnostic value (Cross et al. 2007; Suresh 2007).

Bastatas et al. (2012) used a combination of AFM cell stiffness measurements and cell-substrate adhesion studies, together with calcium imaging and migration studies to investigate prostate cancer metastasis. The Young's modulus was found to be larger for more metastatic cells, in contrast but also in keeping with other studies, suggesting that mechanical studies cannot be used solely as a biomarker for metastasis. Indeed, a complicated relationship is found with adhesion and calcium dynamics also playing important key roles.

Quantitative Imaging® (JPK Instruments), a rapid tip modulation technique that acquires nanomechanical / adhesion data simultaneously with topography, was used by Chopinet et al. (2013) to investigate a number of different cell types, some of which had very little adhesion to the substrate. Force-volume elasticity and adhesion maps could be obtained rapidly and at high resolution for weakly adhered cells. Heu et al. (2012) used PeakForce Tapping® (Bruker), similar to Quantitative Imaging® for rapidly obtaining nanomechanical data at high resolution, to study the increase in stiffness of HaCaT keratinocytes (as a model for skin cancer) brought about through exposure to the herbicide glyphosate. A concentration dependence was observed and the addition of quercetin, a common flavonoid considered to provide protection against oxidative injury and inflammation (Wang et al. 2010), reversed this process.

2.8 Bacteria and bacterial biofilms

There are numerous reports on the use of AFM for investigating bacteria and bacterial biofilms. A few recent highlights are provided here.

Emerson and Camesano (2004) investigated the adhesion of pathogenic microorganisms, *Candida parapsilosis* and *Pseudomonas aeruginosa* (chosen for their clinical relevance), to biomaterials including the *P. aeruginosa* biofilm to unmodified silicone rubber. The attractive force between *C. parapsilosis*, adhered to a probe tip, and a bare silicon substrate was 4.3 ± 0.25 nN, comparable to the smaller attractive forces between *C. parapsilosis* and the *P. aeruginosa* biofilm (2.0 ± 0.4 nN), although the tip experienced repulsive forces 75 nm away from the biofilm surface (2.0 nN). The magnitude of the attractive forces, both towards silicone rubber and the biofilm, led the authors to suggest that they may allow adhesion and colonisation of these surfaces which, in a clinical setting, would increase the risk of death and disease.

The adhesion of *E. coli* to modified silicones using SEM and AFM was investigated by Cao et al. (2006). Their aim was to find a bacteria-resistant surface by varying hydrophobicity through modification. Octadecyltrichlorosilane (OTS) and fluoroalkylsilane (FAS) were tested against hydrophilic mica, which acted as a bacteria-adhesive control surface. Adhesion was investigated by adhering *E. coli* cells to the AFM probe tip and force measurements were taken for the approach to and retraction from surfaces. With the FAS silicone, as with *C. parapsilosis* and the *P. aeruginosa* biofilm (Emerson and Camesano 2004), a repulsive force was observed at close proximity and the force required to remove the tip was low. In contrast, however, when the tip was coated with heparin the attractive forces to FAS were high on both

approach and retraction. This led the authors to conclude that hydrophobicity of a material alone is not enough to predict bacterial adhesion.

Lau et al. (2009) used 'microbead force spectroscopy (MBFS)' to investigate the viscoelasticity of biofilms. A glass bead coated with biofilm was attached to a tip-less cantilever and used as a probe against a flat glass surface. The properties of a *P. aeruginosa* wild-type biofilm were compared with a lipopolysaccharide (LPS)-deficient mutant strain, wapR. Biofilms at different levels of maturity were also compared. When immature, the wapR strain adhered to the glass slide with far more force than the immature wild-type (ranges of 2 - 13 nN and 0 - 3 nN, respectively). As they matured, adhesion forces decreased in both strains. AFM has also been used for investigating real-time visualisation of the antibiotic azithromycin with various lipid domains in solution (Berquand et al. 2004).

2.9 Viruses

Viruses consist of an oligomeric protein head, called a capsid, which contains the viral genome; in more complex virus structures, the capsid may also contain other macromolecules, such as proteins and molecular motors (Martinez-Martin et al. 2012; Mateu 2013). A full historical account of the development of AFM studies of viruses has been reviewed in depth by Baclayon et al. (2010); some highlights are provided in this section. AFM was first used to image viruses in 1992, almost immediately after the instruments became commercially available (Thundat et al. 1992), although these studies were mostly confined to exploiting their well-defined geometry to measure AFM tip radii. An interest in the biological structure of viruses, however, soon followed, with contact mode imaging of head and tail components of bacteriophage T4 (Kolbe et al. 1992). Tapping Mode® in liquid rapidly became the mode of preference, due to reduced lateral forces (Bushell et al. 1995) and a more relevant imaging environment (Kuznetsov et al. 2001), although contact mode is still widely used (Mateu 2013). Topography imaging has been used to distinguish capsomers, determine the triangulation number (T) of capsids (Kuznetsov and McPherson 2011), revealing exposed nucleic acids subsequent to capsid stripping (Drygin et al. 1998; Kienberger et al. 2004; Plomp et al. 2002) and to observe viral budding from living fibroblast cells (Gladnikoff and Rousso 2008). Treatment of pinostroin, an antiviral, was shown to cause severe disruption to HSV-1 virus morphology, as evidenced from topography and phase imaging (Wu et al. 2011).

In addition to imaging, force vs. distance curves, both tip approach (indentation) and tip retract (adhesion) cycles, have been acquired from immobilised viruses. Head, collar and tail regions of ϕ 29 phage virions were found to exhibit different elasticity values (Melcher et al. 2009). A decrease in Young's modulus (stiffness) was reported for *E. coli* after infection with M13 (Chen et al. 2009). Concerning adhesion events, spatially-resolved force mapping was used to examine single influenza virus particles (glycoprotein hemagglutinin, HA, surface) using an anti-HA derivatised tip (Liu et al. 2012).

Recent developments in high-speed AFM imaging at high resolution offer even greater opportunities for studying dynamic virus-cell interactions (Ando et al. 2008).

3. AFM combined with optical or spectroscopic techniques

In the last couple of years, instruments that combine AFM with spectroscopic techniques, such as IR and Raman, and / or improved light microscopy for studying cells conveniently in physiological medium have been made commercially available. These instruments offer considerable potential for in vitro studies, where high-resolution imaging can be combined with biochemical measurements. A few examples are provided here.

Dazzi et al. (2012) showed there to be excellent agreement between conventional IR spectroscopy with nanoscale combined AFM-IR data from polymer samples. By combining AFM imaging with mid-IR spectroscopy, Van Eerdenbrugh et al. (2012) examined the micro- and nanostructure and chemical phase composition of felodipine / poly(acrylic acid) blends. Oil inclusions in streptomyces, without the need for staining, were mapped using a combined AFM-IR instrument by Deniset-Besseau et al. (2014). A high-speed AFM for nano / mesoscale analysis of living cell surfaces (HeLa and 3T3 fibroblasts) has been combined with fluorescence microscopy (Suzuki et al. 2013). High-resolution fluorescence imaging (super resolution stimulated emission depletion, STED) has been combined with nanomechanical (stiffness) mapping to investigate COS-7 cells with immunolabelled microtubuli (Harke et al. 2012). Cell biological aspects such as dynamics of mitochondrial movement and drug uptake have also been investigated (Matthaus et al. 2007).

4. Summary

AFM is a high-resolution imaging technique that can be used to study a variety of samples under physiologically relevant conditions. The ability to chemically or biologically functionalise AFM probes combined with various modes that permit the acquisition of spatially-resolved force data allows for the study of systems at the single-molecule level. AFM technology, now frequently using high-speed acquisition, interfaced with spectroscopic modes and light microscopy methods for live cell imaging offer huge potential for the pharmaceutical sciences.

Appendix: Obtaining an AFM contact mode image in air

As a practical demonstration, this section outlines a typical sequence of the steps necessary for the acquisition of the simplest of AFM operations: a contact mode image to be obtained in air. Most of the details that make the sequence particularly relevant for a particular instrument have deliberately been excluded. Bacteria on a mica surface has been chosen as a suitable sample. Mica is an ideal substrate for many AFM studies since it is atomically flat (glass coverslips can appear quite rough for many high-resolution studies); fresh, uncontaminated surfaces can be also prepared, without the need for cleaning, by simply attaching adhesive tape and peeling away the top layer from this layered material (Morris et al. 2001). Mica is negatively charged and so improved adhesion to often negatively charged biological specimens, such as DNA, can be achieved by derivatising the mica surface with a suitable polycation, e.g., poly-L-lysine (Eaton and West 2010).

1. Turn on the AFM instrument and computer, and open the software.
2. Place a piece of mica (1 cm², cut with scissors) on a nickel stub (1.2 cm²) using double-sided adhesive tape. Press it on firmly.
3. Cleave the mica with adhesive tape. Derivatise the mica, if required.
4. Add an aliquot (10 µL) of the solution containing bacteria to the mica surface. Leave the drop of solution in place for 2 mins.

5. Carefully rinse the treated mica plate with distilled water to remove buffer salts, which might mask any biological sample features.
6. Allow to air-dry or carefully use a jet of nitrogen gas.
7. Place the sample on top of the AFM scanner; the magnet will hold the nickel disc of the sample in place.
8. Select a contact mode probe (of low spring constant k , ca. 0.06 N m^{-1}) and fix into AFM head above the sample.
9. Line up the laser (according to manufacturer's instructions).
10. Move the sample and / or probe to select imaging region of interest.
11. Select a required scan range (say, $20 \mu\text{m}$) and set the scan rate to 1 Hz. Use an image resolution size of at least 512×512 pixels. Select the integral, proportional and derivative (PID, external scanner feedback; Eaton and West 2010) settings outlined by the manufacturer (these will depend mostly on the scanner being used and whether air or liquid is the medium).
12. Lower the probe to just above the sample surface and use the automated approach.
13. Slowly increase the PID settings to maximise image contrast to just below the level that produces noise (piezo ringing). It should also be possible to reduce the applied load (reduce deflection) on the cantilever to improve image quality.
14. Once image settings are optimised, obtain a complete image and save (capture) it.
15. The next typical options will either be to zoom in, move to a different area or change the sample.

References

- Abendan RS, Swift JA (2005) Dissolution on cholesterol monohydrate single-crystal surfaces monitored by in situ atomic force microscopy. *Cryst Growth Des* 5:2146-2153
- Adamcik J, Mezzenga R (2012) Study of amyloid fibrils via atomic force microscopy. *Curr Opin Colloid Interface Sci* 17:369-379
- Ando T, Uchihashi T, Kodera N, Yamamoto D, Miyagi A, Taniguchi M, Yamashita H (2008) High-speed AFM and nano-visualization of biomolecular processes. *Pfluegers Arch Eur J Physiol* 456:211-225
- Antonio PD, Lasalvia M, Perna G, Capozzi V (2012) Scale-independent roughness value of cell membranes studied by means of AFM technique. *Biochim Biophys Acta* 1818:3141-3148
- Arora S, Rajwade JM, Paknikar KM (2012) Nanotoxicology and in vitro studies: The need of the hour. *Toxicol Appl Pharmacol* 258:151-165
- Baclayon M, Wuite GJL, Roos, WH (2010) Imaging and manipulation of single viruses by atomic force microscopy. *Soft Matter* 6:5273-5285
- Bastatas L, Martinez-Martin D, Matthews J, Hashem J, Lee YJ, Sennoune S, Filleur S, Martinez-Zaguilan R, Park S (2012) AFM nano-mechanics and calcium dynamics of prostate cancer cells with distinct metastatic potential. *Biochim Biophys Acta* 1820:1111-1120

Begat P, Morton DAV, Staniforth JN, Price R (2004) The cohesive-adhesive balances in dry powder inhaler formulations I: direct quantification by atomic force microscopy. *Pharm Res* 21:1591-1597

Belletti D, Tonelli M, Forni F, Tosi G, Vandelli MA, Ruozzi B (2013) AFM and TEM characterization of siRNAs lipoplexes: A combinatory tools to predict the efficacy of complexation. *Colloids Surfaces A: Physicochem Eng Aspects* 436:459-466.

Berquand A, Mingeot-Leclercq MP, Dufrene YF (2004) Real-time imaging of drug-membrane interactions by atomic force microscopy. *BBA-Biomembranes* 1664:198-205

Bianco A, Kostarelos K, Prato M (2005) Applications of carbon nanotubes in drug delivery. *Curr Opin Chem Biol* 9:674-679

Binnig G, Rohrer H (1982) Scanning tunnelling microscopy. *Helv Phys Acta* 55:726-735

Binnig G, Quate CF, Gerber C (1986) Atomic force microscope. *Phys Rev Lett* 56:930-933

Bushell GR, Watson GS, Holt SA, Myhra S (1995) Imaging and nano-dissection of tobacco virus by atomic force microscopy. *J Microsc* 180:174-181

Butt HJ, Cappella M, Kappl M (2005) Force measurements with the atomic force microscope: technique, interpretation and applications. *Surf Sci Rep* 59:1-152

Cail TL, Hochella MF (2005) Experimentally derived sticking efficiencies of microparticles using atomic force microscopy. *Environ Sci Technol* 39:1011-1017

Cao T, Tang H, Liang X, Wang A, Auner GW, Salley SO, Ng KYS (2006) Nanoscale investigation on adhesion of E.coli to surface modified silicone using atomic force microscopy. *Biotechnol Bioeng* 94:167-176

Cappella B, Dietler G (1999) Force-distance curves by atomic force microscopy. *Surf Sci Rep* 34:1-104

Chen YY, Wu CC, Hsu JL, Peng L, Chang HY, Yew TR (2009) Surface rigidity change of Escherichia coli after filamentous bacteriophage infection. *Langmuir* 25:4607-4614

Chinnapongse SL, MacCuspie RI, Hackley VA (2011) Persistence of singly dispersed silver nanoparticles in natural freshwaters, synthetic seawater, and simulated estuarine waters. *Sci Total Environ* 409:2443-2450

Chiti F, Dobson CM (2006) Protein misfolding, functional amyloid, and human disease. *Annu Rev Biochem* 75:333-366

Chopinet L, Formosa C, Rols MP, Duval RE, Dague (2013) Imaging living cells surface and quantifying its properties at high resolution using AFM in QI™ mode. *Micron* 48:26-33

Chow EHH, Bucar D-K, Jones W (2012) New opportunities in crystal engineering – the role of atomic force microscopy in studies of molecular crystals. *Chem Commun* 74:9210-9226

Clifford CA, Seah MP (2005) The determination of atomic force microscope cantilever spring constants via dimensional methods for nanomechanical analysis. *Nanotechnol* 16:1666-1680

Couston RG, Lamprou DA, Uddin S, van der Walle C (2012) Interaction and destabilization of a monoclonal antibody and albumin to surfaces of varying functionality and hydrophobicity. *Int J Pharm* 438:71-80

Csontos I, Ronaszegi K, Szabo A, Keszei S, Anna P, Fekete P, Marosi G, Nagy T (2006) Controlled technology for forming a nanostructured polymer coating for solid pharmaceuticals. *Polym Adv Technol* 17:884-888

Craig GE, Brown SD, Lamprou DA, Graham D, Wheate NJ (2012) Cisplatin-tethered gold nanoparticles that exhibit enhanced reproducibility, drug loading, and stability: a step closer to pharmaceutical approval? *Inorg Chem* 51:3490-3497

Cross SE, Jin YS, Rao J, Gimzewski JK (2007) Nanomechanical analysis of cells from cancer patients. *Nature Nanotechnology* 2:780-783

Danesh A, Chen X, Davies MC, Roberts CJ, Sanders GHW, Tendler SJ, Williams PM (2000) Polymorphic discrimination using atomic force microscopy: distinguishing between two polymorphs of the drug cimetidine. *Langmuir* 16:866-870

Danesh A, Connell SD, Davies MC, Roberts CJ, Tendler SJ, Williams PM, Wilkins MJ (2001) An in situ dissolution study of aspirin crystal planes (100) and (001) by atomic force microscopy. *Pharm Res* 18:299-303

Dazzi A, Prater CB, Hu Q, Chase DB, Rabolt JF, Marcott C (2012) AFM-IR: combining atomic force microscopy and infrared spectroscopy for nanoscale chemical characterization. *Appl Spectrosc* 66:1365-1384

Deniset-Besseau A, Prater CB, Virolle M-J, Dazzi A (2014) Monitoring triacylglycerols accumulation by atomic force microscopy based infrared spectroscopy in streptomyces species for biodiesel applications. *J Phys Chem Lett* 5:654-658

Donaldson K, Stone V, Tran CL, Kreyling W, Borm PJA (2004). *Nanotoxicology*. *Occup Environ Med* 61:727-728

Drygin YF, Bordunova OA, Gallyamov MO, Yaminsky IV (1998) Atomic force microscopy examination of tobacco mosaic virus and virion RNA. *FEBS Lett* 425:217-221

Durbin SD, Carlson WE (1992) Lysozyme crystal growth studied by atomic force microscopy. *J Cryst Growth* 122:71-79

Eaton P, West P (2010) *Atomic force microscopy*. Oxford University Press, Oxford

Ebner A, Chtcheglova LA, Preiner J, Tang J, Wildling L, Gruber HJ, Hinterdorfer P (2010) Simultaneous topography and recognition imaging. *Scanning Probe Microscopy in Nanoscience and Nanotechnology NanoScience and Technology*, pp 325-362

Edwardson JM, Henderson RM (2004) Atomic force microscopy and drug discovery. *Drug Discov Today* 9:64-71

Emerson RJ IV, Camesano TA (2004) Nanoscale investigation of pathogenic microbial adhesion to biomaterials. *Appl Environ Microbiol* 70:6012-6022

Fahs A, Louarn G (2013) Plant protein interactions studied using AFM force spectroscopy: nanomechanical and adhesion properties. *Phys Chem Chem Phys* 15:11339-11348

Florin EL, Moy VT, Gaub HE (1994) Adhesion forces between individual ligand-receptor pairs. *Science* 264:415-417

Gladnikoff M, Rouso I (2008) Directly monitoring individual retrovirus budding events using atomic force microscopy. *Biophys J* 94:320-326

Grama CN, Venkatpurwar VP, Lamprou DA, Kumar RMNV (2013) Towards scale-up and regulatory shelf-stability testing of curcumin encapsulated polyester nanoparticles. *Drug Deliv Translat Res* 3:286-293

Harke B, Chacko JV, Haschke H, Canale C, Diaspro A (2012) A novel nanoscopic tool by combining AFM with STED microscopy. *Optical Nanoscopy* 1:1-6

Heu C, Berquand A, Elie-Caille C, Nicod L (2012) Glyphosate-induced stiffening of HaCaT keratinocytes, a peak force tapping study on living cells. *J Struct Biol* 178:1-7

Hinterdorfer P, Baumgartner W, Gruber HJ, Schilcher K, Schindler H (1996) Detection and localization of individual antibody-antigen recognition events by atomic force microscopy. *Proc Natl Acad Sci USA* 93:3477-3481.

Janowski M, Bulte JWM, Walczak P (2012) Personalized nanomedicine advancements for stem cell tracking. *Adv Drug Deliv Rev* 64:1488-1507

Josef A, Mezzenga R (2012) Study of amyloid fibrils via atomic force microscopy. *Curr Opin Colloid Interface Sci* 17:369-376

Kao F-S, Ger W, Pan Y-R, Yu H-C, Hsu R-Q, Chen H-M (2012) Chip-based protein-protein interaction studied by atomic force microscopy. *Biotechnol Bioeng* 109:2460-2467

Karagkiozaki V, Logothetidis S, Vavoulidis E (2012) Nanomedicine pillars and monitoring nanobio-interactions, in: S Logothetidis (Ed.), *Nanomedicine and Nanobiotechnology*, Springer, Heidelberg, pp. 27-52.

Karagkiozaki V, Karagiannidis PG, Gioti M, Kavatzikidou P, Georgiou D, Georgarakis E, Logothetidis S (2013) Bioelectronics meets nanomedicine for cardiovascular implants: PEDOT-based nanocoatings for tissue regeneration. *Biochim Biophys Acta* 1830:4294-4304

Kienberger F, Zhu R, Moser R, Blaas D, Hinterdorfer P (2004) Monitoring RNA release from human rhinovirus by dynamic force microscopy. *J Virol* 78:3203-3209

Kolbe WF, Ogletree DF, Salmeron MB (1992) Atomic force microscopy imaging of T4 bacteriophages on silicon substrates. *Ultramicroscopy* 42-44:1113-1117

Kozlova EK, Chernysh AM, Moroz VV, Kuzovlev AN (2013) Analysis of nanostructure of red blood cells membranes by space fourier transform of AFM images. *Micron* 44:218-227

Kuznetsov YG, Malkin AJ, Lucas RW, Plomp M, McPherson A (2001) Imaging of viruses by atomic force microscopy. *J Gen Virol* 82:2025-2034

Kuznetsov YG, McPherson A (2011) Atomic force microscopy in imaging of viruses and virus-infected cells. *Microbiol Mol Biol Rev* 75:268-285

Lamprou DA, Smith JR, Nevell TG, Barbu E, Willis CR, Tsibouklis J (2010) Self-assembled structures of alkanethiols on gold-coated cantilever tips and substrates for atomic force microscopy: molecular organisation and conditions for reproducible deposition. *Appl Surf Sci* 256:1961-1968

Lamprou DA, Venkattapurwar V, Kumar MNVR (2013) Atomic force microscopy images label-free, drug encapsulated nanoparticles in vivo and detects difference in tissue mechanical properties of treated and untreated: a tip for nanotoxicology. *PLoS ONE* 8: e64490

Land TA, De Yoreo JJ (2000) The evolution of growth modes and activity of growth sources on canavalin investigated by in situ atomic force microscopy. *J Cryst Growth* 1-4:623-637

Lau PCY, Lindhout T, Beveridge TJ, Dutcher JR, Lam JS (2009) Differential lipopolysaccharide core capping leads to quantitative and correlated modifications of mechanical and structural properties in pseudomonas aeruginosa biofilms. *J Bacteriol* 191:6618-6631

Levy G (1961) Comparison of dissolution and absorption rates of different commercial aspirin tablets. *J Pharm Sci* 50:388-392

Li QS, Lee GYH, Ong CN, Lim CT (2008) AFM indentation study of breast cancer cells. *Biochem Biophys Res Commun* 374:609-613

Li M, Liu L, Xi N, Wang Y, Dong Z, Xiao X, Zhang W (2013a) Atomic force microscopy imaging of live mammalian cells. *Sci China Life Sci* 56:811-817

Li M, Xiao X, Liu L, Xi N, Wang Y, Dong Z, Zhang W (2013b) Nanoscale mapping and organization analysis of target proteins on cancer cells from B-cell lymphoma patients. *Exp Cell Res* 319:2812-2821.

Liu C-H, Horng J-T, Chang J-S, Hsieh C-F, Tseng Y-C, Lin S (2012) Localization and force analysis at the single virus particle level using atomic force microscopy. *Biochem Biophys Res Commun* 417:109-115

Mains J, Lamprou DA, McIntosh L, Oswald IDH, Urquhart AJ (2013) Beta-adrenoceptor antagonists affect amyloid nanostructure; amyloid hydrogels as drug delivery vehicles. *Chem Commun* 49:5082-5084

Mao H, Chen W, Laurent S, Thirifays C, Burtea C, Rezaee F, Mahmoudi M (2013) Hard corona composition and cellular toxicities of the graphene sheets. *Colloids Surfaces B: Biointerfaces* 109:212-218

Martinez-Martin D, Carrasco C, Hernando-Perez M, de Pablo PJ, Gomez-Herrero J, Perez R, Mateu MG, Carrascosa JL, Kiracofe D, Melcher J, Raman A (2012) Resolving structure and mechanical properties at the nanoscale of viruses with frequency modulated atomic force microscopy. *PLoS One* 7:e30204

Mateu MG (2013) Assembly, stability and dynamics of virus capsids. *Arch Biochem Biophys* 531:65-79

Matthaus C, Chernenko T, Newmark JA, Warner CM, Diem M (2007) Label-free detection of mitochondrial distribution in cells by nonresonant Raman microspectroscopy. *Biophys J* 93:668-673

McPherson A, Malkin AJ, Kuznetsov YG, Plomp M (2001) Atomic force microscopy applications in macromolecular crystallography. *Acta Crystallogr D Biol Crystallogr* 57:1053-1060

Melcher J, Carrasco C, Xu X, Carrascosa JL, Gomez-Herrero J, de Pablo JD, Raman A (2009) Origins of phase contrast in the atomic force microscope in liquids. *Proc Natl Acad Sci USA* 106:13655-13660

Miyazaki T, Aso Y, Kawanishi T (2011) Feasibility of atomic force microscopy for determining crystal growth rates of nifedipine at the surface of amorphous solids with and without polymers. *J Pharm Sci* 100:4413-4420

Morris VJ, Kirby AR, Gunning AP (2001) *Atomic force microscopy for biologists*, Imperial College Press, London

Muller DJ, Helenius J, Alsteens D, Dufrene YF (2009) Force probing surfaces of living cells to molecular resolution. *Nat Chem Biol* 5:383-390

Onuma K, Ito A, Tateishi T, Kameyama T (1995) Surface observations of synthetic hydroxyapatite single crystal by atomic force microscopy. *J Cryst Growth* 148:201-206

Onyesom I, Lamprou DA, Sygellou L, Owusu-Ware SK, Antonijevic M, Chowdhry BZ, Douroumis D (2013) Sirolimus encapsulated liposomes for cancer therapy: physicochemical and mechanical characterization of sirolimus distribution within liposome bilayers. *Mol Pharmaceutics* 10:4281-4293

Potta SG, Minemi S, Nukala RK, Peinado C, Lamprou DA, Urquhart AJ, Douroumis D (2011) Preparation and characterization of ibuprofen solid lipid nanoparticles with enhanced solubility. *J Microencapsul* 28:74-81

Plomp M, Rice MK, Wagner EK, McPherson A, Malkin AJ (2002) Rapid visualization at high resolution of pathogens by atomic force microscopy: structural studies of herpes simplex virus-1. *Am J Pathol* 160:1959-1966

Riener CK, Strohm CM, Ebner A, Klampfl C, Gall AA, Romania C, Lyubchenko YL, Hinterdorfer P, Gruber HJ (2003) Simple test system for single molecule recognition force microscopy. *Anal Chim Acta* 479:59-75

Roberts CJ (2005) What can we learn from atomic force microscopy adhesion measurements with single drug particles? *Eur J Pharm Sci* 24:153-157

Roldo M, Power K, Smith JR, Cox PA, Papagelis K, Bouropoulos N, Fatouros DG (2009) N-Octyl-O-sulfate chitosan stabilises single wall carbon nanotubes in aqueous media and bestows biocompatibility. *Nanoscale* 1:366-373

Romer M, Heinamaki J, Strachan C, Sandler N, Yliruusi J (2008) Prediction of tablet film-coating thickness using a rotating plate coating system and NIR spectroscopy. *AAPS Pharm Sci Tech* 9:1047-1053

Schmitz I, Schreiner M, Friedbacher G, Grasserbauer M (1997) Phase imaging as an extension to tapping mode AFM for the identification of material properties on humidity-sensitive surfaces. *Appl Surf Sci* 115:190-198

Seitavuopio P, Rantanen J, Yliruusi J (2003) Tablet surface characterisation by various imaging techniques. *Int J Pharm* 254:281-286

Seitavuopio P, Rantanen J, Yliruusi J (2005) Use of roughness maps in visualisation of surfaces. *Eur J Pharm Biopharm* 59:351-358

Seitavuopio P, Heinamaki J, Rantanen J, Yliruusi J (2006) Monitoring tablet surface roughness during the film coating process. *AAPS Pharm Sci Tech* 7:E1-E6

Sikora AE, Smith JR, Campbell SA and Firman F (2012) AFM protein-protein interactions within the EcoR124I molecular motor. *Soft Matter* 8:6358-6363

Sitterberg J, Ozcetin A, Ehrhardt C, Bakowsky U (2010) Utilising atomic force microscopy for the characterisation of nanoscale drug delivery systems. *Eur J Pharm Biopharm* 74:2-13

Smith DA, Connell SD, Kirkham CR (2003a) Chemical force microscopy: applications in surface characterisation of natural hydroxyapatite. *Anal Chim Acta* 479:39-57

Smith JR, Breakspear S, Campbell SA (2003b) AFM in surface finishing: Part 2 Surface roughness. *Trans IMF* 81:B55-B58

Smith JR, Lamprou DA (2014) Polymer coatings for biomedical applications: a review. *Trans IMF* 92:9-19

Song Y, Bhushan B (2006) Dynamic analysis of torsional resonance mode of atomic force microscopy and its application to in-plane surface property extraction. *J Microsyst Technol* 12:219-230

Suresh S (2007) Nanomedicine - Elastic clues in cancer detection. *Nature Nanotechnol* 2:748-749

Suzuki Y, Sakai N, Yoshida A, Uekusa Y, Yagi A, Imaoka Y, Ito S, Karaki K, Takeyasu K (2013) High-speed atomic force microscopy combined with inverted optical microscopy for studying cellular events. *Sci Rep* 3:2131

Tasis D, Papagelis K, Douroumis D, Smith JR, Bouropoulos N, Fatouros DG (2008) Diameter-selective solubilization of carbon nanotubes by lipid micelles. *J Nanosci Nanotechnol* 8:420-423

Tetard L, Passian RH, Farahi RH, Thundat T (2010) Atomic force microscopy of silica nanoparticles and carbon nanohorns in macrophages and red blood cells. *Ultramicroscopy* 110:586-591

Thakuria R, Eddleston MD, Chow EHH, Lloyd GO, Aldous BJ, Krzyzaniak JF, Bond AD, Jones W (2013) Use of in situ atomic force microscopy to follow phase changes at crystal surfaces in real time. *Angew Chem Int Ed* 52:10541-10544

Theodoropoulos D, Rova A, Smith JR, Barbu E, Calabrese G, Vizirianakis IS, Tsibouklis J, Fatouros DG (2013) Towards boron neutron capture therapy: the formulation and preliminary in vitro evaluation of liposomal vehicles for the therapeutic delivery of the dequalinium salt of bis-nido-carborane. *Bioorg Med Chem Lett* 23:6161-6166

Thio BJR, Zhou D, Keller AA (2011) Influence of natural organic matter on the aggregation and deposition of titanium dioxide nanoparticles. *J Hazard Mater* 189:556-563

Thompson C, Davies MC, Roberts CJ, Tendler SJ, Wilkinson MJ (2004) The effects of additives on the growth and morphology of paracetamol (acetaminophen) crystals. *Int J Pharm* 280:137-150

Thundat T, Zheng XY, Sharp SL, Allison DP, Warmack RJ, Joy DC, Ferrell TL (1992) Calibration of atomic force microscope tips using biomolecules. *Scanning Microsc* 6:903-910

Tonglei L, Kenneth RM, Kinam P (2000) Influence of solvent and crystalline supramolecular structure on the formation of etching patterns on acetaminophen single crystals: a study with atomic force microscopy and computer simulation. *J Phys Chem B* 104:2019-2032

Tsukada M, Irie R, Yonemochi Y, Noda R, Kamiya H, Watanabe W, Kauppinen EI (2004) Adhesion force measurement of a DPI size pharmaceutical particle by colloid probe atomic force microscopy. *Powder Technol* 141:262-269

Van Eerdenbrugh B, Lo M, Kjoller K, Marcott C, Taylor LS (2012) Nanoscale mid-infrared imaging of phase separation in a drug-polymer blend. *J Pharm Sci* 101:2066-2073

Wang XY, He PY, Du J, Zhang JZ (2010) Quercetin in combating H₂O₂ induced early cell apoptosis and mitochondrial damage to normal human keratinocytes. *Chinese Med J* 123:532-536

Wise JA, Smith JR, Bouropoulos N, Yannopoulos SN, van der Merwe SM, Fatouros DG (2008) Single wall carbon nanotube dispersions stabilised with N-trimethyl-chitosan. *J Biomed Nanotechnol* 4:67-72

Wu N, Kong Y, Zu Y, Fu Y, Liu Z, Meng R, Liu X, Efferth T (2011) Activity investigation of pinostrobin towards herpes simplex virus-1 as determined by atomic force microscopy. *Phytomed* 18:110-118

Xue W-F, Hellewell AL, Gosal WS, Homans SW, Hewitt EW, Radford SE (2009) Fibril fragmentation enhances amyloid cytotoxicity. *J Biol Chem* 284:34272-34282

Yip CM, Ward MD (1996) Atomic force microscopy of insulin single crystals: direct visualization of molecules and crystal growth. *Biophys J* 71:1071-1078

Zhang W, Stack AG, Chen Y (2011) Interaction force measurement between E. coli cells and nanoparticles immobilized surfaces by using AFM. *Colloids Surfaces B: Biointerfaces* 82:316-324

Pre-print